Journal of Materials Chemistry C

PAPER

View Article Online
View Journal | View Issue

Cite this: J. Mater. Chem. C, 2014, 2, 1801

Twisted intramolecular charge transfer, aggregation-induced emission, supramolecular self-assembly and the optical waveguide of barbituric acid-functionalized tetraphenylethene†

Erjing Wang,[ab] Jacky W. Y. Lam,[ab] Rongrong Hu,[ab] Chuang Zhang,[c] Yong Sheng Zhao[c] and Ben Zhong Tang*[abd]

Received 1st November 2013
Accepted 10th December 2013

DOI: 10.1039/c3tc32161d

www.rsc.org/MaterialsC

A red-emissive barbituric acid-functionalized tetraphenylethene derivative (TPE-HPh-Bar) was designed and synthesized. TPE-HPh-Bar exhibits the effect of twisted intramolecular charge transfer due to the interaction of its donor and acceptor units. Whereas TPE-HPh-Bar emits faintly in solution, it becomes a strong emitter in the aggregated state, demonstrating a phenomenon of aggregation-induced emission. TPE-HPh-Bar can self-assemble into nanospheres upon natural evaporation of its solutions. In the presence of melamine, nanorods and (un)sealed nanotubes are formed, the content of which depends on the melamine amount. The crystalline nanorods of TPE-HPh-Bar grown from diethyl ether/hexane solution exhibit a good optical waveguiding effect with a low optical loss (0.137 dB μm^{-1}). Such attributes make the material to find wide applications in many areas such as biological imaging and optoelectronic nano-devices.

Introduction

In 2001, Tang discovered the phenomenon of aggregation-induced emission (AIE),[1] which is exactly opposite to the aggregation-caused quenching (ACQ) effect observed in some conventional fluorophores.[2,3] For example, hexaphenylsilole and tetraphenylethene (TPE) are non-luminescent when molecularly dissolved in solutions, but become highly emissive in the aggregated state. The restriction of intramolecular motion (RIM) in the aggregated state is responsible for such a phenomenon. Such a discovery changes people's way of thinking about the light emitting process in the aggregated state and has attracted much interest among scientists. More than 100 research groups in the world are now doing AIE research. Their enthusiastic efforts have generated a large number and a wide variety of AIE luminogens with potential high-technological applications. Most of the AIE luminogens prepared so far emit blue and green light. For biological applications, especially in whole animal and deep tissue imaging,[4] dye molecules with longer-wavelength emissions are preferred because they suffer no interference from the auto-fluorescence of biological tissues. There are two ways to acquire such dyes. One methodology is the extension of the molecular π conjugation so as to narrow the energy band gap for electronic transitions. However, this strategy possesses the disadvantages of tedious synthesis, high synthetic workload, ease of induction of emission quenching owing to strong intermolecular interaction, susceptible photo-oxidation and poor dye solubility. The other way is to introduce electron donating (D) and withdrawing (A) units into the molecular structure. Dye molecules with such donor–acceptor structures form charge transfer states with a narrow band gap in polar solvents,[5] thus red-shifting the emission to longer wavelengths.

Studies on micro- and nano-materials and related devices are hot topics in modern nanoscience and nanotechnology. Thanks to their strong solid-state emission, AIE luminogens are found to be promising materials for fabricating optoelectronic devices with micro-dimensions.[3,6] Fabrication of micro- and nano-devices from AIE molecules and studies on their field emission and optical waveguide properties, however, are rarely reported.[7] Tang and coworkers introduced a mesogenic unit between two TPE units, and the resulting molecules can self-assemble into

[a]HKUST-Shenzhen Research Institute, No. 9. Yuexing 1st RD, South Area, Hi-tech Park, Nanshan, Shenzhen, 518057, China. E-mail: tangbenz@ust.hk

[b]Department of Chemistry, Institute of Molecular Functional Materials and Institute for Advanced Study, The Hong Kong University of Science & Technology (HKUST), Clear Water Bay, Kowloon, Hong Kong, China

[c]Beijing National Laboratory for Molecular Sciences, Key Laboratory of Photochemistry, Institute of Chemistry, Chinese Academy of Sciences, Beijing 100190, China

[d]Guangdong Innovative Research Team, SCUT-HKUST Joint Research Laboratory, State Key Laboratory of Luminescent Materials and Devices, South China University of Technology (SCUT), Guangzhou 510640, China

† Electronic supplementary information (ESI) available: ^{1}H NMR and ^{13}C NMR spectra of TPE-HPH-Bar and its precursor, PL spectra in the dichloromethane/hexane mixture and SEM images obtained from acetonitrile solution and the DMSO/ethanol mixture. See DOI: 10.1039/c3tc32161d

highly fluorescent (helical) nanofibers.[8] They also studied the self-assembly behaviours of silole derivatives, which can form crystalline microfibers and further microrods from their THF/ethanol solutions.[9] Tian reported the nano-ring structures of AIE-active anthracene derivatives formed from THF/water mixtures.[10] While conditions and mechanisms for the formation of these self-assembly morphologies have been discussed, their opto-electronic properties have not been studied in detail.

A previous study has shown that non-covalent interactions such as hydrogen bonding, π–π stacking, and electrostatic interactions are the main driving forces for self-assembly to ordered micro- and nano-structures.[11] The mode of self-assembly, on the other hand, can be realized by tuning the physical conditions such as temperature, concentration, time, and addition order of different solutions. Recently, Zheng published a TPE macrocycle, which can facilely self-assemble into crystalline and hollow spheres with both intrinsic and extrinsic pores. Ultrasonic treatment on the hollow spheres can transform them into bird nests consisting of nanorods.[12]

Another way to tune the self-assembly behaviour is to utilize the co-assembly effect of different compositions. In this strategy, the addition of another composition can induce the former to self-assemble into a more ordered structure so as to improve the morphology and modify the physical and chemical properties.[13] One good example is the pair of melamine and barbituric acid, whose self-assembly behaviours have been studied for decades due to their strong hydrogen bonding between molecules.[14] Zhang utilized hydrochloric acid and triethylamine to control the self-assembly behaviour of melamine and alkylated melamine. The chloride ion connects the melamine molecules by forming hydrogen bonds with their amino groups and changes the morphologies from 3D networks to 2D micro-sheets.[15] Researchers also utilized the strong interaction between melamine and barbituric acid to sense melamine in food and milk.[16] Sanji functionalized TPE with cyauric acid, a counterpart of barbituric acid with a similar structure, and utilized the resulting luminogen to detect melamine in milk by virtue of the AIE property of TPE.[17]

Herein, we report the synthesis and self-assembly behaviour of a TPE derivative functionalized with barbituric acid (TPE-HPh-Bar; Scheme 1). The luminogen exhibits the characteristics of both AIE and twisted intramolecular charge transfer (TICT). The strong D–A effect endows TPE-HPh-Bar with red emission. TPE-HPh-Bar is also capable of self-assembling into nanospheres by slow evaporation of its pure acetonitrile solution or nanorods and nanotubes from different solvent systems in the presence of melamine. Its microrods exhibit optical waveguiding properties with a low optical loss. Such results make TPE-HPh-Bar have an array of optoelectronic and biological applications.

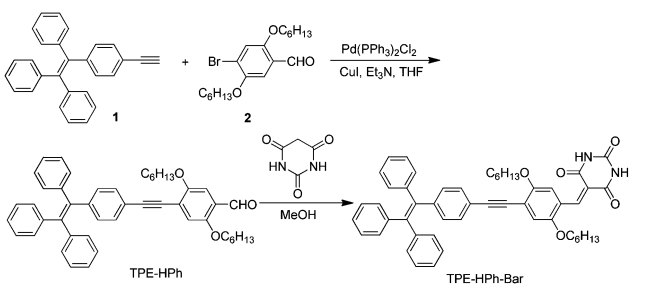

Scheme 1 Synthetic route to TPE-HPh-Bar.

Experimental section

Materials

Tetrahydrofuran (THF) was distilled from a sodium benzophenone system in a nitrogen atmosphere under normal pressure immediately prior to use. Triethylamine was dried using potassium hydroxide pellets. Other solvents, such as diethyl ether, *n*-hexane, dichloromethane (DCM), methanol and dimethyl sulfoxide (DMSO), were of high purity and used as received. 2-(4-Ethynylphenyl)-1,1,2-triphenylethene (**1**) was synthesized according to our previously reported procedures.[18] 4-Bromo-2,5-bis(hexyloxy)benzaldehyde (**2**) was synthesized from hydroquinone using the literature method.[19] Other reagents such as bis(triphenylphosphine)palladium(II) chloride, triphenylphosphine, cuprous iodide, liquid bromine, *n*-butyllithium and *N*-formylpiperidine were purchased from commercial companies and used directly without further purification.

Instruments

^{1}H and ^{13}C NMR spectra were measured on a Bruker ARX 400 spectrometer using deuterated chloroform as solvent and tetramethylsilane (TMS) as an internal standard. High-resolution mass spectra (HRMS) were recorded on a GCT premier CAB048 mass spectrometer operated in a MALDI-TOF mode. Elemental analysis was performed on an Elementar Vario EL Elemental Analyzer. Absorption spectra were taken on a Milton Roy Spectronic 3000 Array spectrometer. Photoluminescence (PL) spectra were taken on a Perkin-Elmer LS 55 spectrofluorometer. The PL quantum yield of the solid powder was determined using a calibrated integrating sphere. Scanning electron microscopy (SEM) images were obtained on a JOEL 6390 SEM instrument. The SEM samples were prepared by drop-casting the dye solution onto silicon substrates. The solvent was evaporated at room temperature in the air. For samples prepared from dye solution in dimethyl sulfoxide, they were further dried under vacuum overnight. To measure the microarea PL spectra of the crystalline microrods of TPE-HPh-Bar obtained from its diethyl ether/hexane mixture, the microrods were dispersed on a glass coverslip and excited with a UV laser (λ = 400 nm, Beamlok, Spectraphysics). The excitation laser was filtered with a band-pass filter (400–450 nm) and then focused to excite the microrod with a suitable objective. The collected PL emission was coupled to a grating spectrometer (Acton, SP-2358) with a matched ProEm: 512B EMCCD camera (Princeton Instruments).

Synthesis

2,5-Bis(hexyloxy)-4-{[4-(1,2,2-triphenylvinyl)phenyl]ethynyl}-benzaldehyde (TPE-HPh). To a two-neck round-bottom flask were added 2-(4-ethynylphenyl)-1,1,2-triphenylethene **1** (1 g, 2.81 mmol), 4-bromo-2,5-bis(hexyloxy)benzaldehyde **2** (1.03 g,

2.68 mmol), bis(triphenylphosphine)palladium(II) chloride (0.089 g, 0.126 mmol), cuprous iodide (0.024 g, 0.121 mmol) and triphenylphosphine (0.066 g, 0.251 mmol). The reaction mixture were degassed and purged with nitrogen three times, after which freshly distilled THF (30 mL) and dry triethylamine (10 mL) were injected *via* syringes. The reaction mixture was stirred under reflux at 70 °C for 8 h. After cooling to room temperature, the formed precipitate was filtered and the solvent was removed under vacuum. The crude product was purified on a silica-gel column using hexane/dichloromethane (4 : 1 v/v) as an eluent to afford the product as a yellow solid. Yield 73.4% (1.3 g). ^{1}H NMR (400 MHz, $CDCl_3$): δ (TMS, ppm) 10.44 (s, 1H), 7.30 (d, 2H), 7.27 (s, 1H), 7.15–7.08 (m, 9H), 7.06 (s, 1H), 7.05–7.00 (m, 8H), 4.05–4.00 (m, 4H), 1.87–1.77 (m, 4H), 1.50–1.46 (m, 4H), 1.37–1.31 (m, 8H), 0.93–0.85 (m, 6H). ^{13}C NMR (100 MHz, $CDCl_3$): δ (TMS, ppm) 189.42, 155.73, 153.82, 144.74, 143.63, 143.58, 143.47, 142.07, 140.38, 131.61, 131.58, 131.53, 131.50, 131.32, 128.04, 127.98, 127.88, 126.92, 126.85, 124.90, 120.92, 120.81, 117.48, 110.06, 97.80, 85.98, 69.53, 69.41, 31.74, 31.70, 29.32, 25.92, 25.88, 22.81, 22.79, 14.25, 14.23. HRMS (MALDI-TOF): *m*/*z* 660.3596 (M^+, calcd 660.3603). M.p.: 99.3–100.2 °C.

TPE-HPh-Bar. To a round-bottom flask were added TPE-HPh (500 mg, 0.758 mmol) and barbituric acid (106 mg, 0.828 mmol) in 40 mL of methanol. The mixture was stirred and heated to reflux under nitrogen for 24 h. The formed red precipitates were filtered while hot and washed with methanol three times. The red solid was dissolved in diethyl ether, after which an appropriate amount of hexane was added. The resulting mixture was left for recrystallization to acquire needle-like crystals in 61% yield (0.356 g) ^{1}H NMR (400 MHz, $CDCl_3$): δ (TMS, ppm) 9.06 (s, 1H), 8.30 (s, 1H), 8.18 (s, 1H), 8.11 (s, 1H), 7.29 (d, 2H), 7.13–7.08 (m, 9H), 7.05–7.01 (m, 8H), 6.98 (s, 1H), 4.06–4.02 (m, 4H), 1.86–1.81 (m, 4H), 1.58–1.43 (m, 4H), 1.37–1.29 (m, 8H), 0.92–0.84 (m, 6H). ^{13}C NMR (100 MHz, $CDCl_3$): δ (TMS, ppm) 163.06, 161.00, 155.25, 154.63, 152.73, 148.88, 144.92, 143.59, 143.48, 142.17, 140.40, 131.65, 131.59, 131.54, 131.50, 131.44, 128.06, 128.00, 127.90, 126.95, 126.88, 122.15, 116.88, 115.68, 114.89, 98.85, 86.66, 69.80, 69.69, 31.80, 31.67, 29.38, 29.24, 25.96, 25.85, 22.82, 22.78, 14.26, 14.21. HRMS (MALDI-TOF): *m*/*z* 770.3722 (M+, calcd 770.3720). Anal. calcd for $C_{51}H_{50}N_2O_5$: C, 79.45; H, 6.54; N, 3.63. Found: C, 79.60; H, 6.606; N, 3.59. M.p.: 189.0–190.1 °C.

Preparation of nanoaggregates

Stock THF and dichloromethane solutions of TPE-HPh-Bar with a concentration of 200 μM were prepared. Aliquots of the stock solution were transferred to 10 mL volumetric flasks. After appropriate amounts of THF or dichloromethane were added, water or hexane was added dropwise under vigorous stirring to furnish 10 μM solutions with different water or hexane fractions (0–95 vol%). PL measurements of the resulting solutions were then carried out immediately.

Results and discussion

Scheme 1 shows the synthetic route to TPE-HPh-Bar. Sonogashira cross-coupling of **1** and **2** catalysed by $Pd(PPh_3)_2Cl_2$ and CuI in a THF/Et_3N mixture afforded TPE-HPh in a yield of above 70%. TPE-HPh has a moderate solubility in common organic solvents such as THF, chloroform, dichloromethane and acetone. Reaction of TPE-HPh with barbituric acid in methanol under reflux produced the final product TPE-HPh-Bar.[20] All the compounds were characterized by standard spectroscopic methods, from which satisfactory analysis data corresponding to their molecular structures were obtained. TPE-HPh-Bar was obtained as a red solid and possessed better solubility than TPE-HPh in common solvents. Besides, TPE-HPh-Bar has a good solubility in diethyl ether.

Optical properties

Fig. 1 shows the UV spectra of TPE-HPh and TPE-HPh-Bar in pure THF solutions. The absorption maxima of TPE-HPh and TPE-HPh-Bar are located at 388 nm and 447 nm with molar absorptivities of 2.63 × 10^5 L mol^{-1} cm^{-1} and 2.99 × 10^5 L mol^{-1} cm^{-1}, respectively, which are 63 nm and 122 nm red shifted from that of TPE owing to the extended conjugation as well as the TICT effect.[21] The formation of the D–A structure will narrow the energy band gap for electronic transitions, as reflected by the red-shift UV absorption and PL emission. Since the polarity of water is much higher than that of THF, increasing the water content leads to higher polarity of the solvent system and thus red-shifts the emission due to the TICT attribute.[5] Owing to that the spectroscopic property of TICT molecules is sensitive to environmental polarity, the TICT portrait of molecules can be verified through spectroscopic measurement. From Fig. S5,† it can be seen that with increased solvent polarity, both UV absorption and PL emission red-shift. The emission changes from about 545 nm in diethyl ether to 590 nm in methanol. Because of the higher electron-withdrawing character of the barbituric acid unit than the aldehyde group, the D–A interaction in TPE-HPh-Bar is stronger than that in TPE-HPh, thus leading to larger red-shift in the absorption maximum. The dilute THF solution (10 μM) of TPE-HPh-Bar

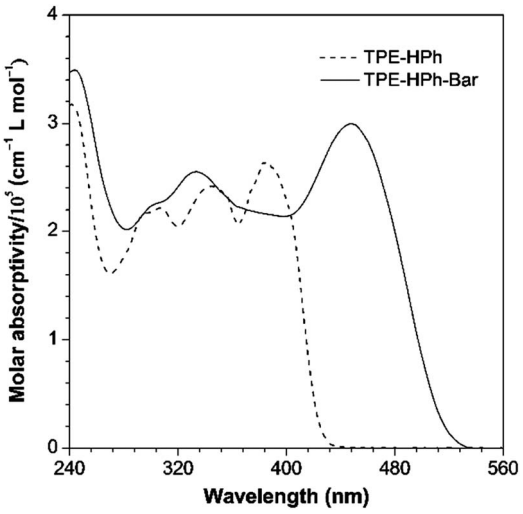

Fig. 1 UV-vis spectra of TPE-HPh and TPE-HPh-Bar in pure THF solutions.

shows a yellow emission at 545 nm upon UV irradiation. To check whether TPE-HPh-Bar is AIE-active, we added water, a non-solvent for TPE-HPh-Bar, into its THF solution and examined the PL change. When the water fraction was gradually increased to 60 vol%, the emission from the solution was weakened progressively. Afterwards, the PL intensity starts to rise and reaches its maximum at 80% water fraction (Fig. 2). Below 60% water fraction, the molecules do not form sufficient aggregates, and the TICT effect dominates the emission behaviour: since water is more polar than THF, with increase in water content, the increased polarity will induce intensity-reduced and red shifted emission. Above 60% water fraction, the AIE effect overwhelms the TICT effect, and as a whole, the emission begins to increase and TPE-HPh-Bar mainly shows the AIE effect. Further increment of the water fraction has, however, decreased slightly the light emission. On the other hand, the PL spectrum shifts progressively to the redder region with increasing the water content. At 90% water fraction, the PL maximum is located at 630 nm, which is 100 nm red-shifted from that in pure THF solution. Such PL change is not unusual and has been observed in some AIE-active luminogens with D–A structures. With a gradual increase in the water content, the polarity of the THF/water mixture becomes higher. This strengthens the TICT effect and thus weakens and red-shifts the light emission of TPE-HPh-Bar. At water content higher than 60%, the solving power of the solvent mixture becomes so poor that it induces the TPE-HPh-Bar molecules to aggregate. This activates the AIE process and hence enhances the light emission. The slight drop in PL intensity at high water content is due to the precipitation of the large-sized aggregates, which decreases the effective dye concentration in the solution. To diminish the TICT effect on the AIE process, we repeated the PL measurement in DCM with a less polar solvent of hexane. The addition of hexane has little influence on the polarity of the whole system, thus eliminating the polarity effect. As shown in Fig. S6,† the PL intensity gradually increases with increasing the hexane fraction. Meanwhile, the emission maximum blue shifts from 587 nm in DCM to 538 nm in the DCM/hexane mixture with 95% hexane fraction. This result truly verifies the AIE characteristics of TPE-HPh-Bar. Therefore, TPE-HPh-Bar shows TICT plus AIE characteristics in the highly polar THF/H_2O mixture and typical AIE characteristics in the less polar dichloromethane/hexane mixture. The solid-state quantum yield of TPE-HPh-Bar determined by an integrating sphere is 37.4%, which is quite high among the red-emissive semiconductors. This makes TPE-HPh-Bar promising for the fabrication of optoelectronic devices.

Self-assembly

Self-assembly is an efficient bottom-up method to form materials with ordered micro- and nano-structures or even supramolecular structures. Interestingly, upon natural evaporation of a few drops of acetonitrile solution of TPE-HPh-Bar on the silicon substrate, nanospheres are formed. The nanospheres are uniform with size tunable by the solution concentration (Fig. 3 and Fig. S7†). The higher the concentration, the larger is the size of the formed nanospheres. Addition of ethanol or water into the acetonitrile solution causes no change in the self-assembly morphology, but the size of the nanoparticles becomes smaller at the same experimental conditions. For example, to achieve the same particle size of 500 nm, an acetonitrile/ethanol mixture (1 : 1 v/v) with a concentration of 50 μM should be used, which is five times more concentrated than that of the acetonitrile solution. Even smaller-sized nanospheres are obtained from the acetonitrile/water mixture (1 : 1 v/v). Since ethanol and water are both poor solvents for TPE-HPh-Bar, addition of these solvents into its acetonitrile solution will aggregate its molecules quickly, leading to the formation of nanospheres with small sizes. We then investigated the effect of melamine on the self-assembly behavior of TPE-HPh-Bar. Instead of nanospheres, nanorods are formed from acetonitrile solution containing melamine (Fig. 4), whose fraction increases with increasing the amount of melamine in the solution. Some tubular structures are also formed at the

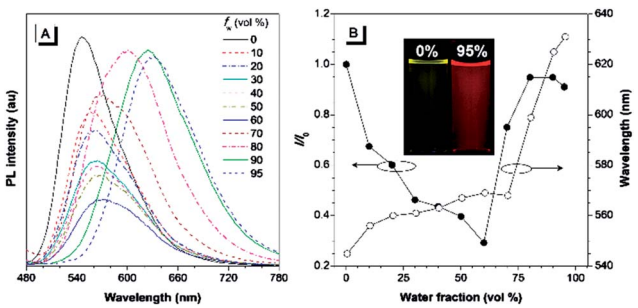

Fig. 2 (A) PL spectra of TPE-HPh-Bar in THF/water mixtures with different water fractions (f_w). Concentration: 10 μM; excitation wavelength: 447 nm. (B) Plot of relative PL intensity (I/I_0) and the emission maximum *versus* the composition of the THF/water mixture of TPE-HPh-Bar. I_0 = emission intensity in pure THF solution. Inset: fluorescent photographs of TPE-HPh-Bar in THF/water mixtures with water fractions of 0% and 95% taken under UV irradiation.

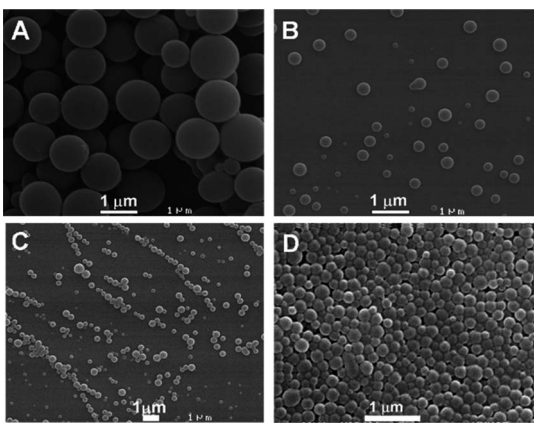

Fig. 3 (A and B) SEM images of micro- and nano-spheres formed by slow evaporation of TPE-HPh-Bar solution in acetonitrile with concentrations of (A) 100 μM and (B) 10 μM. (C and D) SEM image of nanospheres formed by slow evaporation of TPE-HPh-Bar solution (50 μM) in (C) acetonitrile/ethanol and (D) acetonitrile/water mixtures (1 : 1 v/v) at room temperature.

same time. Some papers proposed the transition mechanism from nanorods and nano-sheets to nanotubes,[22] in which the melamine molecules induce an ordered arrangement of TPE-HPh-Bar through intermolecular hydrogen bonding in certain dimensions.

Since acetonitrile is not a good solvent for melamine, only part of the TPE-HPh-Bar molecules can interact with the melamine molecules. Thus, we used DMSO as solvent for the morphology study as melamine has good solubility in this solvent. However, its low volatility requires us to modify the self-assembly process. First, a DMSO solution of TPE-HPh-Bar was prepared and an appropriate amount of melamine solution in DMSO was then added. The resulting mixture was left at room temperature for some times, after which ethanol was added. The mixture was then dropped on the silicon substrate to allow solvent evaporation under ambient conditions. As the molecular size of TPE-HPh-Bar is much larger than melamine, a higher relative amount of melamine was used to enable complete interaction between the two molecules. In the presence of 10 equivalents of melamine, nanotubes with lengths of about 30 μm and diameters of about 50 nm are formed from the DMSO/ethanol mixture (1 : 1 v/v) (Fig. 5). Most of the ends of the tubes are not sealed, presumably due to the etching effect of DMSO. Such morphology is rarely observed in adducts of barbituric acid and melamine. Increasing the melamine amount to 25 equivalents exerts little change on the thickness of nanorods but has sealed the tube ends. Besides, other solvent systems including 1,4-dioxane, THF, CH_3CN, CH_3CN/H_2O, and CH_3CN/ethanol were used to study the self-assembly behaviour. In most cases, nanosphere structures are obtained in the absence of melamine. But with the addition of melamine, rods will form in the solvents (see Fig. S9†).

We also studied the self-assembly morphology by TEM but observed no such micro- and nano-structures, probably due to the different sample preparation procedure. When the volume ratio of DMSO to ethanol is changed from 1 : 1 to 1 : 4 v/v, the micro- and nano-structures become smaller and irregular (Fig. S8†). The TPE-HPh-Bar molecules will aggregate in the solvent mixture with a large amount of ethanol, thus impeding their co-assembly with the melamine molecules. Lowering the DMSO content, on the other hand, has diminished the etching effect, which may have an adverse effect on the formation of opened nanotubes. The good self-assembly capability of TPE-HPh-Bar makes it to find wide applications in micro- and nano-devices such as light transmission and field emission.

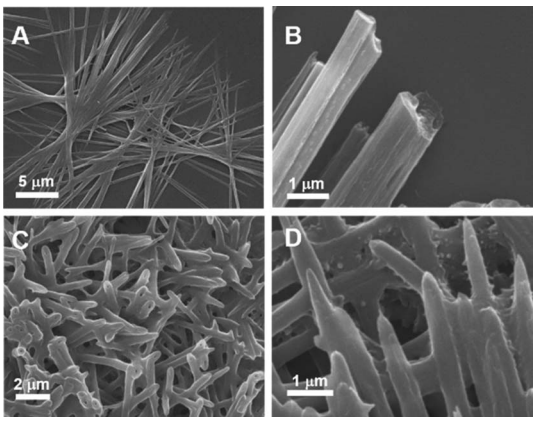

Fig. 5 SEM images of micro- and nano-aggregates formed by slow evaporation of TPE-HPh-Bar solution (10 μM) in the DMSO/ethanol mixture (1 : 1 v/v) at room temperature in the presence of (A and B) 10 and (C and D) 25 equivalents of melamine.

Optical waveguide

TPE-HPh-Bar can facilely self-assemble into crystalline microrods from the diethyl ether/hexane mixture, as revealed by the X-ray diffraction and the fluorescent photograph shown in Fig. 6. However, their sizes are too small to be analysed by single crystal X-ray diffraction. We tried to grow better samples in other solvent systems such as chloroform, acetonitrile, and chloroform/pentane and chloroform/hexane mixtures but failed to obtain any suitable specimen. Nevertheless, the appropriate length and regular shape of the microrods encourage us to study their optical wave-guiding properties.[23] As suggested by the fluorescent photograph shown in Fig. 7A, the nanorod surface shows no obvious defect. When the

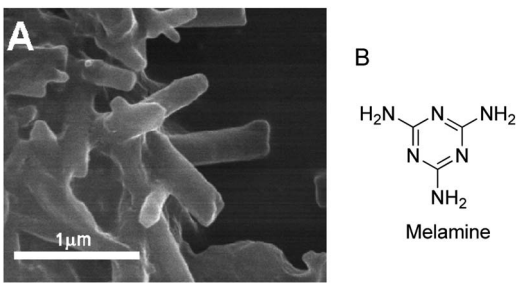

Fig. 4 (A) SEM image of micro-aggregates formed by slow evaporation of TPE-HPh-Bar solution in acetonitrile (10 μM) in the presence of 1 equivalent of melamine at room temperature. (B) Chemical structure of melamine.

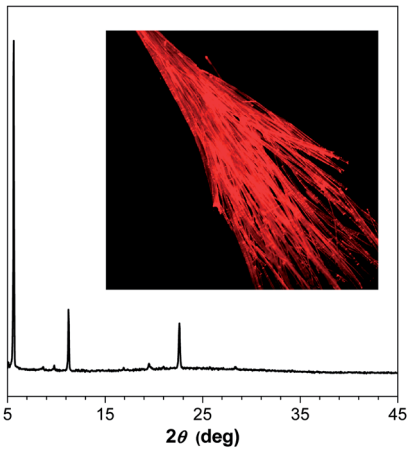

Fig. 6 X-ray diffractogram of microrods of TPE-HPh-Bar formed from the diethyl ether/hexane mixture. Inset: fluorescent photograph of TPE-HPh-Bar microrods taken under UV irradiation.

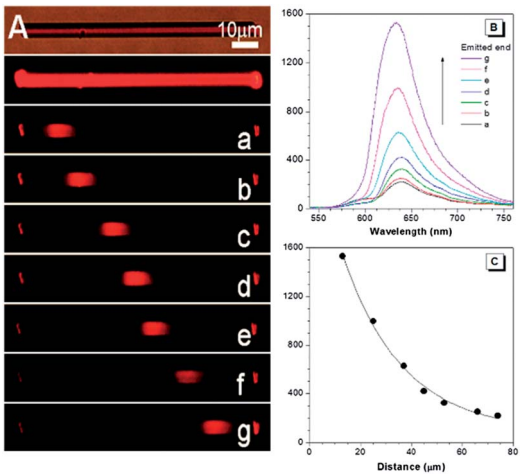

Fig. 7 (A) Microarea fluorescent images of the TPE-HPh-Bar microrod obtained by exciting at seven different positions with a focused UV laser (400 nm); (B) spatially resolved PL spectra of the TPE-HPh-Bar microrod recorded at the right rod ends labelled with a–g in 7A; (C) plot of peak intensity *versus* the distance between the excited sites and the emitted ends.

microrod was excited by 400 nm UV light produced by an 800 nm laser device at different positions, the emission was detected at the rod end, whose intensity becomes lower when the excitation spot moves gradually to the opposite rod end (Fig. 7B). By plotting its intensity (I_{end}) and its distance to the irradiated area (x), the optical loss coefficient (α) was calculated by using a single exponential fitting [$I_{end}/I_{ex} = A\exp^{-\alpha x}$, where I_{ex} is the PL intensity at the excited spot and A is the ratio of the light escaped from the excited area and that propagated along the fiber][24] and was determined to be 0.137 dB μm^{-1} (Fig. 7C). This value is quite low among the red-emissive AIE-active luminogens reported so far.[25] The partial overlapping between the absorption and emission spectra is one of the factors to diminish the optical wave-guiding effect.[26] The large Stokes shift (~100 nm) and the smooth and flat end facets of TPE-HPh-Bar crystals help in minimizing the optical loss, thus contributing to their good optical wave-guiding behaviours. Applications of TPE-HPh-Bar in micro/nano-laser[27] and spectral modulation[28] are currently being carried out in our laboratory.

Conclusion

A red-emissive barbituric acid-functionalized TPE derivative, TPE-HPh-Bar, was designed and synthesized. TPE-HPh-Bar exhibits both the TICT effect and the AIE phenomenon. It can self-assemble into nanospheres through slow evaporation of its acetonitrile solution. In the presence of melamine, nanorods and (un)sealed nanotubes are generated. The crystalline microrods of TPE-HPh-Bar grown from diethyl ether/hexane solution show a good optical waveguiding effect with a low optical loss. Such attributes make TPE-HPh-Bar have wide applications in many areas such as biological imaging and optoelectronic nano-devices.

Acknowledgements

The work reported in this paper was partially supported by the National Basic Research Program of China (973 program, 2013CB834701), the Research Grants Council of Hong Kong (HKUST2/CRF/10 and N_HKUST620/11), and the University Grants Committee of Hong Kong (AoE/P-03/08 and T23-713111-1), and B. Z. Tang thanks the support of the Guangdong Innovative Research Team Program (201101C0105067115).

Notes and references

1 J. Luo, Z. Xie, J. W. Y. Lam, L. Cheng, H. Chen, C. Qiu, H. S. Kwok, X. Zhan, Y. Liu, D. Zhu and B. Z. Tang, *Chem. Commun.*, 2001, 1740.
2 (*a*) Y. Hong, J. W. Y. Lam and B. Z. Tang, *Chem. Commun.*, 2009, 4332; (*b*) Y. Hong, J. W. Y. Lam and B. Z. Tang, *Chem. Soc. Rev.*, 2011, **40**, 5361.
3 Z. Zhao, J. W. Y. Lam and B. Z. Tang, *J. Mater. Chem.*, 2012, **22**, 23726.
4 V. J. Pansare, S. Hejazi, W. J. Faenza and R. K. Prud'homme, *Chem. Mater.*, 2012, **24**, 812.
5 (*a*) M. Shigeta, M. Morita and G. Konishi, *Molecules*, 2012, **17**, 4452; (*b*) A. Maliakal, G. Lem, N. J. Turro, R. Ravichandran, J. C. Suhadolnik, A. D. DeBellis, M. G. Wood and J. Lau, *J. Phys. Chem. A*, 2002, **106**, 7680.
6 (*a*) W. Z. Yuan, P. Lu, S. Chen, J. W. Y. Lam, Z. Wang, Y. Liu, H. S. Kwok, Y. Ma and B. Z. Tang, *Adv. Mater.*, 2010, **22**, 2159; (*b*) Y. Liu, S. Chen, J. W. Y. Lam, P. Lu, R. T. K. Kwok, F. Mahtab, H. S. Kwok and B. Z. Tang, *Chem. Mater.*, 2011, **23**, 2536; (*c*) B.-K. An, S. H. Gihm, J. W. Chung, C. R. Park, S.-K. Kwon and S. Y. Park, *J. Am. Chem. Soc.*, 2009, **131**, 3950; (*d*) B.-K. An, D.-S. Lee, J.-S. Lee, Y.-S. Park, H.-S. Song and S. Y. Park, *J. Am. Chem. Soc.*, 2004, **126**, 10232.
7 (*a*) Z. Zhao, J. W. Y. Lam and B. Z. Tang, *Soft Matter*, 2013, **9**, 4564; (*b*) A. Patra and U. Scherf, *Chem.–Eur. J.*, 2012, **18**, 10074.
8 W. Z. Yuan, F. Mahtab, Y. Gong, Z.-Q. Yu, P. Lu, Y. Tang, J. W. Y. Lam, C. Zhu and B. Z. Tang, *J. Mater. Chem.*, 2012, **22**, 10472.
9 Z. Zhao, S. Chen, X. Shen, F. Mahtab, Y. Yu, P. Lu, J. W. Y. Lam, H. S. Kwok and B. Z. Tang, *Chem. Commun.*, 2010, **46**, 686.
10 B. Xu, J. He, Y. Dong, F. Chen, W. Yu and W. Tian, *Chem. Commun.*, 2011, **47**, 6602.
11 L. Maggini and D. Bonifazi, *Chem. Soc. Rev.*, 2012, **41**, 211.
12 S. Song and Y.-S. Zheng, *Org. Lett.*, 2013, **15**, 820.
13 (*a*) H. Y. Lee, S. R. Nam and J.-I. Hong, *J. Am. Chem. Soc.*, 2007, **129**, 1040; (*b*) W. Yang, Y. Jiang, J. Zhuang, N. Lü, S. Chen and T. Li, *Sci. China, Ser. B: Chem.*, 2001, **44**, 478; (*c*) J. Gao, Y. He, H. Xu, B. Song, X. Zhang, Z. Wang and X. Wang, *Chem. Mater.*, 2007, **19**, 14.
14 (*a*) Q. Feng, M. Wang, B. Dong, C. Xu, J. Zhao and H. Zhang, *CrystEngComm*, 2013, **15**, 3623; (*b*) H. Koyano, K. Yoshihara, K. Ariga, T. Kunitake, Y. Oishi, O. Kawano, M. Kuramori and K. Suehiro, *Chem. Commun.*, 1996, 1769.

15 J. Xu, G. Wu, Z. Wang and X. Zhang, *Chem. Sci.*, 2012, **3**, 3227.
16 H. Huang, D. Xiang, L. Li, H. Li, G. Zeng and Z. He, *Chem. J. Chin. Univ.*, 2011, **32**, 2504.
17 T. Sanji, M. Nakamura, S. Kawamata, M. Tanaka, S. Itagaki and T. Gunji, *Chem.–Eur. J.*, 2012, **18**, 15254.
18 R. Hu, J. L. Maldonado, M. Rodriguez, C. Deng, C. K. W. Jim, J. W. Y. Lam, M. M. F. Yuen, G. Ramos-Ortiz and B. Z. Tang, *J. Mater. Chem.*, 2012, **22**, 232.
19 H.-C. Lin, M.-D. Jiang, S.-C. Wu, L.-L. Jou, K.-P. Chou, C.-M. Huang and K.-H. Wei, *J. Polym. Sci., Part A: Polym. Chem.*, 2009, **47**, 4685.
20 B. S. Jursic, *J. Heterocycl. Chem.*, 2001, **38**, 655.
21 (*a*) Z. R. Grabowski, K. Rotkiewicz and W. Rettig, *Chem. Rev.*, 2003, **103**, 3899; (*b*) K. Bhattacharyya and M. Chowdhury, *Chem. Rev.*, 1993, **93**, 507.
22 (*a*) N. Chandrasekhar and R. Chandrasekar, *Chem. Commun.*, 2010, **46**, 2915; (*b*) H. Tang, J. P. Gao, Y. Xiong and Z. Y. Wang, *Cryst. Growth Des.*, 2006, **6**, 1559; (*c*) Y. S. Zhao, W. Yang, D. Xiao, X. Sheng, X. Yang, Z. Shuai, Y. Luo and J. Yao, *Chem. Mater.*, 2005, **17**, 6430; (*d*) J. C. MacDonald and G. M. Whitesides, *Chem. Rev.*, 1994, **94**, 2383.
23 C. Zhang, Y. S. Zhao and J. Yao, *Phys. Chem. Chem. Phys.*, 2011, **13**, 9060.
24 T. Liu, Y. Li, Y. Yan, Y. Li, Y. Yu, N. Chen, S. Chen, C. Liu, Y. Zhao and H. Liu, *J. Phys. Chem. C*, 2012, **116**, 14134.
25 (*a*) C. Shi, Z. Guo, Y. Yan, S. Zhu, Y. Xie, Y. S. Zhao, W. Zhu and H. Tian, *ACS Appl. Mater. Interfaces*, 2013, **5**, 192; (*b*) X. Wang, Y. Zhou, T. Lei, N. Hu, E.-Q. Chen and J. Pei, *Chem. Mater.*, 2010, **22**, 3735; (*c*) Q. Bao, B. M. Goh, B. Yan, T. Yu, Z. Shen and K. P. Loh, *Adv. Mater.*, 2010, **22**, 3661.
26 (*a*) K. Takazawa, Y. Kitahama, Y. Kimura and G. Kido, *Nano Lett.*, 2005, **5**, 1293; (*b*) Y. S. Zhao, J. Xu, A. Peng, H. Fu, Y. Ma, L. Jiang and J. Yao, *Angew. Chem., Int. Ed.*, 2008, **47**, 7301.
27 T. Liu, Y. Li, Y. Yan, Y. Li, Y. Yu, N. Chen, S. Chen, C. Liu, Y. Zhao and H. Liu, *J. Phys. Chem. C*, 2012, **116**, 14134.
28 C. Zhang, C.-L. Zou, Y. Yan, R. Hao, F.-W. Sun, Z.-F. Han, Y. S. Zhao and J. Yao, *J. Am. Chem. Soc.*, 2011, **133**, 7276.